

# Recent advances in optimization of photoanodes and counter electrodes of dye-sensitized solar cells

Saily Bhagwat<sup>1,\*</sup>, Riddhesh Dani<sup>1</sup>, Prerna Goswami<sup>2</sup> and M. A. K. Kerawalla<sup>2</sup>

<sup>1</sup>Department of Chemical Engineering, and

<sup>2</sup>Department of General Engineering, Institute of Chemical Technology, Nathalal Parekh Marg, Matunga, Mumbai 400 019, India

Since 1991, dye-sensitized solar cells (DSSCs) have emerged as a potential alternative to conventional silicon photovoltaics for conversion of solar energy to electric power, due to their advantages of cost-effectiveness, sustainability and ease of fabrication among others. As the functioning of DSSCs depends on the sum of the functions of individual components, effective understanding and optimization of these components is important for the optimization of the device itself. Therefore, this review focuses on the recent developments made in the fabrication of two particular components of DSSCs, viz. photoanode and counter electrode.

**Keywords:** Counter electrode, device optimization, dye-sensitized solar cells, photoanode.

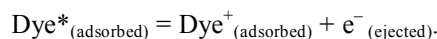
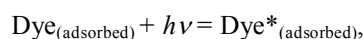
DYE-SENSITIZED solar cells (DSSCs) have been steadily gathering attention in the scientific community ever since Graetzel *et al.*<sup>1</sup> reported energy conversion efficiencies of about 7%–8% with their fabrication. The primary reason to replace conventional silicon-based photovoltaics with DSSCs lies in their sustainability, environment-friendly nature, ease and low cost of fabrication.

As a device, DSSC forms a type of molecular system wherein the sum of the properties of the individual components can be used for a rudimentary prediction of the functioning of the device as a whole<sup>2</sup>. Therefore, effective understanding and optimization of individual components is important for overall optimization of the device. Traditional DSSCs have been structured based on the following four components:

1. A photoanode: This comprises a mesoporous semiconductor oxide film with particle size range in nanometres facilitating electronic transport, supported on a transparent conducting substrate of fluorine-doped tin oxide (FTO). n-Type semiconductors like TiO<sub>2</sub>, SnO<sub>2</sub>, ZnO, etc. have been used in majority of DSSCs, where photoelectrons emitted from the light-harvesting sensitizers are injected in the conduction band of the

semiconductor. Developments in the optimization of the photoanode have been discussed in this article. p-Type semiconductors, wherein positive charges or so-called holes are injected into their valence band from the dye sensitizers have, however, been extremely uncommon and will not be covered detail in this article.

2. A light-harvesting dye sensitizer forming a monolayer on the semiconductor particles: This is central to the photon-to-electron conversion mechanism of the device. Upon photoexcitation, the sensitizer injects electrons into the conduction band of the semiconductor for n-type DSSC (and a hole in its valence band for p-type DSSC), from where it is transferred to the FTO photoanode and then to the external circuit.

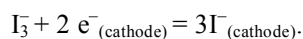
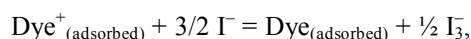


For effective charge transfer in the common n-type DSSCs, the excited state energy level of the dye sensitizer must be higher than the conduction band of the semiconductor. The requirement for a p-type DSSC would, however, be that the highest occupied molecular orbital (HOMO) of the dye sensitizer be at a more positive potential than the valence band of the semiconductor. This process leads to the formation of holes, i.e. positive charges in the dye sensitizer. For continual use of the device, the dye sensitizer has to be regenerated by reduction by the redox electrolyte. For effective regeneration, the oxidized state of the dye sensitizer must have a greater positive value than the redox potential of the electrolyte that is to reduce it.

3. A redox couple in an electrolyte solution: The function of the redox couple is to act as a mediator between the dye sensitizer and the counter electrode. Upon generation of holes in the dye, it is regenerated by reduction with the electrolyte, which itself gets oxidized. The redox electrolyte itself is reduced to its original form by receiving electrons from the counter

\*For correspondence. (e-mail: bsaily361@gmail.com)

electrode (CE) that serves as the cathode of the DSSC.

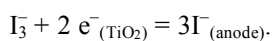
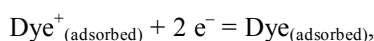


The transport of the redox couple between the photoanode and the CE occurs via diffusion through the electrolyte solution, indicating that the transport of charge inside a DSSC occurs by diffusion of the charge-carrying molecules rather than ‘hopping of charges’ as in semiconductor diodes. Therefore, despite its photochemical activity and corrosive nature, the  $\text{I}^-/\text{I}_3$  couple has been almost ubiquitously used as the redox mediator due to the irreplaceably slow charge recombination reaction, which drives the process in the required direction. Also, as far as the solvent electrolytes that facilitate the movement of the redox couples are concerned, those are mostly polar organic solvents or ionic liquids.

4. Counter electrode: The counter electrode or cathode of DSSCs comprises a catalytic film of platinum (Pt) on a transparent conduction FTO–glass substrate. Pt serves as an electrocatalyst to reduce  $\text{I}_3$  in the redox couple with the electrons that reach it from the external circuit. Several alternatives have been sought to Pt as a material of fabrication of the CE, which are discussed in this article.

Figure 1 shows a schematic of a conventional DSSC.

Besides the reactions mentioned above, there are possibilities of side conversions. These include recombination of photoelectrons with holes in the oxidized dye sensitizers and redirection of electrons from the conduction band of the semiconductor to  $\text{I}_3$  as<sup>3</sup>



These undesired reactions can be prevented by suitable modifications in the photoanode leading to an overall optimization of the device.

The overall conversion in a DSSC is the conversion of the incident solar radiation into electric energy without any permanent chemical change in the components of the DSSC. The energy conversion efficiency,  $\eta$  of the device is directly proportional to the short circuit current or the photocurrent per unit area ( $J_{\text{sc}}$ ), the open circuit voltage ( $V_{\text{oc}}$ ), and the so-called fill factor (FF) of the device, and inversely proportional to the intensity of the incident light ( $I_s$ ), i.e.

$$\eta_{\text{overall}} = (J_{\text{sc}} \times V_{\text{oc}} \times \text{FF}) / (I_s).$$

Here,  $V_{\text{oc}}$  is the potential difference developed in the external circuit on exposure of the DSSC to radiation, and corresponds to the energy difference between the Nerst potential of the redox electrolyte and the Fermi level of the electron in the conduction band of the semiconductor. Also, FF is the ratio of the maximum real power obtained by the device and the theoretical power output possible by the device

$$\text{FF} = P_{\text{max}} / P_{\text{th}}.$$

Recent developments in the fabrication of the photoanodes and CEs are discussed with reference to these parameters.

### Recent developments in photoanode fabrication

Conventional DSSCs have been coated with semiconductor oxide layer of  $\text{TiO}_2$  (anatase). It was preferred due to its easy availability, low toxicity and ease of fabrication of the photoanode with the same, although  $\text{ZnO}$  has also been explored due to its similarly favourable conduction band edge and higher electron mobility. The surface properties and morphology of the photoanode directly affect the overall energy conversion efficiency of DSSC by

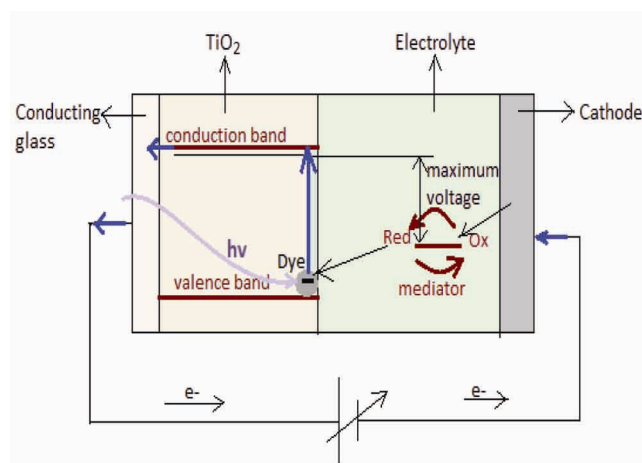


**Figure 1.** Schematic diagram of a conventional dye-sensitized solar cell (DSSC). Flowing line indicates incoming sunlight.

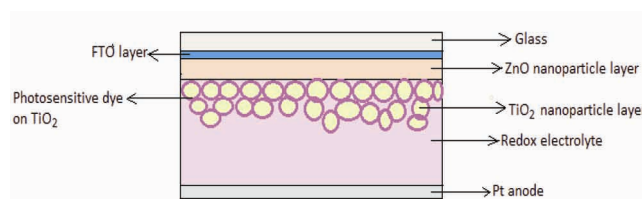


**Figure 2.** Schematic representation of a DSSC with a ZnO–TiO<sub>2</sub> electrode.

influencing the cell parameters of  $J_{sc}$ ,  $V_{oc}$  and FF, and hence these have been a subject of hectic research. In the application of  $TiO_2$  itself, there have been several modifications using various morphologies along with the incorporation of other suitable materials. Kang *et al.*<sup>4</sup> indicated an increase in FF and  $V_{oc}$  of a conventional DSSC by the insertion of a layer of ZnO and Ga-doped ZnO between a layer of  $TiO_2$  nanoparticles and the FTO–glass substrate (Figure 2). The observation was attributed to increased suppression of electron–hole combination and an enhancement in electron transport due to the incorporated ZnO. However, a simultaneous decrement in the  $J_{sc}$  was also observed which was due to the increase in serial resistance because of the additional ZnO layer. However, the two contradicting effects were claimed to have been in favour of an overall increase in the power conversion efficiency (PCE) over a traditional DSSC with other factors being the same. Kang *et al.*<sup>4</sup> also fabricated a new  $TiO_2$  photoanode using nanoporous/nanoparticle  $TiO_2$  layers (Figure 3). Despite a small reduction in the  $J_{sc}$  due to the added resistance of the nanoporous  $TiO_2$ , an enhancement in PCE was found to be attainable. This was attributed to an increase in the scattering path of light, a decrease in the contact resistance between the  $TiO_2$  film and FTO due to its nanostructured nature as well as suppression of the recombination process between the electrons ejected in the FTO with  $I_3^-$  ions in the redox electrolyte.

Mehmood *et al.*<sup>5</sup> fabricated DSSC by incorporation of activated carbon having excellent electronic properties in the  $TiO_2$  photoanode for greater electron mobility. A reduction in the band gap of  $TiO_2$  was found to have resulted due to the addition of AC causing enhanced injection of photoelectrons into the photoanode after their ejection from the dye molecules. The porosity of AC was found to enhance the dye-absorbing ability of the  $TiO_2$  photoanode, resulting in an enhanced photon capture than a similar unmodified DSSC.

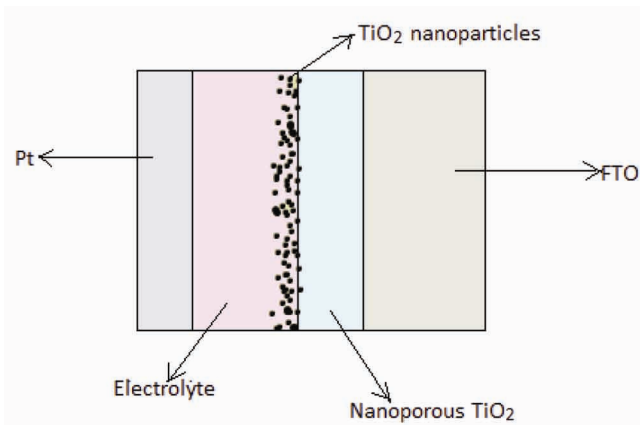


**Figure 3.** Schematic representation of a DSSC with photoanode made from nanoporous nanoparticle  $TiO_2$ .

Graphene, due to some of its interesting properties, has been considered for incorporation in  $TiO_2$  photoanodes. With its two-dimensional structure and zero band gap, graphene tends to treat electrons as massless, relativistic objects leading to an excellent electrical conduction and an improvement in the electron transport. Chou *et al.*<sup>6</sup> incorporated graphene oxide (GO) in  $TiO_2$  and studied the photovoltaic behaviour of the resulting photoanode. With its energy level of  $-4.4$  eV lying between the  $-4.2$  eV conduction band of  $TiO_2$  and the  $-4.7$  eV conduction band of FTO, GO of an optimum concentration causes a reduction in the resistance offered for the transport of the photoelectrons from the dye to the FTO. The DSSC so fabricated showed a PCE value of 5.26%, which was more than that for a similar unmodified DSSC. Recently, Yao *et al.*<sup>7</sup> worked on fabricating photoanodes for DSSCs with reduced interfacial recombination by doping  $TiO_2$  with NiO and  $Eu^{3+}/Tb^{3+}$  to obtain a good efficiency of 8.8%. NiO is a p-type semiconductor with a rather wide band gap with  $E_g = 3.55$  eV, whose combination with the n-type  $TiO_2$  led to the formation of a p–n junction making charge separation effective. The dye molecules were supposed to have adhered effectively to NiO, and the photoelectrons ejected into the conduction band (CB) of NiO were proposed to have been transferred into the CB of  $TiO_2$  via tunnelling mechanism, a process facilitated by  $Eu^{3+}/Tb^{3+}$ . Also, NiO was found to form a barrier layer preventing charge recombination between the  $TiO_2$  film and  $I^-/I_3^-$  electrolyte thus improving  $J_{sc}$  and  $V_{oc}$ , and improving overall PCE. In addition, the  $Eu^{3+}/Tb^{3+}$  dopants were further attributed with suppressing the recombination of charge carriers by causing acceleration in interfacial electron transfer. The resulting efficiency was found to be well above the 6.17% of unmodified DSSCs, suggesting a potential for use of such dopants in  $TiO_2$  photoanodes. Overall, the incorporation of dopants or formation of composites of  $TiO_2$  with other materials has proven to be an effective method for optimization of such photoanodes.

However,  $TiO_2$  reportedly has low stability under ultraviolet (UV) radiation. Also, the low band due to the low band gap of  $TiO_2$  results into generation of electron–hole pairs under UV light, which in turn cause the light-harvesting dye layer on the surface to eventually degrade with time. Therefore, despite their numerous advantages, alternative semi-conductor oxides have been explored for fabrication of DSSC photoanodes. Tin oxide ( $SnO_2$ ) has been identified as a potential candidate with its high band gap energy of 3.62 eV, providing it with higher stability under UV light. It also has an electron mobility of 100–200  $cm^2/V.s$  as opposed to 0.1–1  $cm^2/V.s$  of  $TiO_2$ , giving it an additional advantage over  $TiO_2$ . However, fabrication of photoanodes entirely from  $SnO_2$  has been found to be difficult due to its lesser capacity to load the sensitizing dye molecules. Therefore, efforts have been made towards fabrication of photoanodes with composites of

SnO<sub>2</sub> nanofibers or nanorods with TiO<sub>2</sub>, as these materials have been predicted to enhance charge transport<sup>8</sup>. Song *et al.*<sup>9</sup> found an improvement in the 7.54% PCE of TiO<sub>2</sub> photoanodes by incorporation of SnO<sub>2</sub> nanorods in the TiO<sub>2</sub> particulate films, resulting in a PCE of 8.61%. The SnO<sub>2</sub> nanorods were attributed with a higher intrinsic electron mobility, offering little hindrance to the transport of electrons to the FTO electrode, thus increasing the  $J_{sc}$  and hence the overall PCE. Wang *et al.* fabricated a DSSC photoanode entirely from SnO<sub>2</sub>, by collective employment of several of its different morphologies<sup>10</sup>. They fabricated a double-layered photoanode with the bottom layer comprising SnO<sub>2</sub> nanoparticles (NPs) and the top layer comprising SnO<sub>2</sub> nanofibers (NFs)<sup>10</sup>. The SnO<sub>2</sub> NFs were considered to have served as an efficient light-scattering layer thereby increasing the light-harvesting function while at the same time providing for a linear, direct path for effective collection and transport of electrons through the DSSC. The SnO<sub>2</sub> NPs on the other hand were attributed with lowering charge combination rates at the interface between the FTO–glass electrode and the  $\Gamma/I_3^-$  redox couple. Due to these factors, an overall efficiency of 6.31% was attained by Wang *et al.*<sup>10</sup>. These experiments indicate that if its low absorption tendencies towards the light-harvesting dye molecules are overcome, SnO<sub>2</sub> can be an effective alternative for TiO<sub>2</sub> in DSSC photoanodes.

Besides SnO<sub>2</sub>, ZnO has also been an alternative to TiO<sub>2</sub> in the fabrication of DSSC photoanodes, with efforts directed towards designing photoanodes using ZnO nanoparticles and ZnO nanocrystalline aggregates. Gao *et al.*<sup>11</sup> fabricated ZnO nanocrystalline photoanodes by interface precipitation method which yielded good dye-holding properties through a large specific surface area and a good photocurrent due to effective light scattering within the photoanode. A thorough analysis of recent developments in the application of TiO<sub>2</sub>, SnO<sub>2</sub> and ZnO to DSSC photoanodes, with the focus being on various surface morphologies, has been reviewed by Concina *et al.*<sup>12</sup>.

TiO<sub>2</sub>, SnO<sub>2</sub> and ZnO are all *n*-type DSSCs with very few *p*-type DSSCs being readily fabricated. After photoexcitation of the sensitizer, in *n*-type DSSCs an electron is injected into the conduction band of the semiconductor, whereas in the *p*-type DSSCs a hole is injected in the valence band of the semiconductor. Efforts have been made towards fabricating purely *p*-type DSSCs, such as the manufacture of indium tin oxide (ITO) photoanodes by Yu *et al.*<sup>13</sup>. Despite making use of [Fe(acac)<sub>3</sub>]<sup>0/-</sup> solution as the redox electrolyte, a PCE value of only about 1.96% ( $\pm 0.12\%$ ) was reported. Lack of appropriate *p*-type semiconductors with a suitably wide band gap, sufficient absorptivity of sunlight and sufficient charge transport properties have been considered to be the factors responsible for the current scenario of lack of a feasible *p*-type

DSSC. Introduction of *p*-type DSSCs would depend on the research endeavours directed towards the same.

In addition to the aforementioned *n*-type semiconductors and their composites, several binary and ternary oxides with a band gap energy similar to anatase have also been explored. These include zinc stannate (Zn<sub>2</sub>SnO<sub>4</sub>), niobium pentoxide (Nb<sub>2</sub>O<sub>5</sub>), SrTiO<sub>3</sub> and WO<sub>3</sub>, among others<sup>14</sup>. Despite their properties of high electron mobility, conduction bands comparable or higher than that of TiO<sub>2</sub>, chemical stability and ease of synthesis, the use of such oxides is yet to be on a wide scale. For certain oxides, studies have attributed the poor generation of photocurrents to low loading of the dye sensitizer by the semiconductor, and not due to intrinsic failures of the semiconductor in terms of poor charge transport or electron injection. A more detailed review on the use of such alternative semiconductor oxides can be found in Alibaie *et al.*<sup>14</sup>.

### Recent developments in counter electrode fabrication

Conventionally DSSCs adopted a FTO glass substrate loaded with platinum as counter electrodes, due to the good catalytic activity offered by platinum for iodide/triiodide redox reactions and its high resistance to corrosion relative to other metallic catalysts such as iron, nickel, etc. However, the stability of the FTO-based Pt catalyst was found to vary with the method of fabrication, with reports of generation of PtI<sub>4</sub> due to corrosion by triiodide solutions. Also, although the 50 mg/m<sup>2</sup> standard amount of Pt required for efficient catalytic activity does not significantly increase the price per energy conversion, for the employment of DSSCs on a larger scale in future, a need was felt to seek alternatives to Pt with lower cost and easier availability. There has been exhaustive research over the use of carbonaceous materials such as carbon black, mesoporous carbon (MC), activated carbon, graphite, graphene, carbon nanotubes (CNTs) and the composites of these materials with TiO<sub>2</sub> and other conductive materials for the fabrication of DSSC CEs. Some of these have been reviewed by Kouhnavard *et al.*<sup>15</sup>.

Ramasamy *et al.*<sup>16</sup> fabricated new CEs using multi-walled CNTs. With their highly efficient bamboo-like structures rich in defects, multi-walled CNTs were supposed to facilitate good electron-transfer kinetics while also aiding efficient electrocatalytic reduction of the  $\Gamma/I_3^-$  electrolyte. Due to their large surface area and high electrical conductivity, the multi-walled CNTs were found to make DSSCs with  $V_{oc} = 0.740$  V,  $J_{sc} = 16.2$  mA/cm<sup>2</sup> and FF value of 64%, amounting to an overall 7.67% energy conversion efficiency. These results were found to be comparable to  $V_{oc} = 0.730$  V,  $J_{sc} = 16.5$  mA/cm<sup>2</sup>, FF = 65% and PCE of 7.83% displayed by similar DSSCs with

**Table 1.** Variation of DSSC cell parameters with varying compositions of fabrication

Counter electrode (CE)	CE thickness ( $\mu\text{m}$ )	$J_{\text{sc}}$ ( $\text{mA}/\text{cm}^2$ )	$V_{\text{oc}}$ (V)	FF (%)	$\eta$ (%)
ECN	43	11.98	0.81	54.4	5.28
ECN : CNP (70 : 30)	38.66	13.08	0.77	54.8	5.5
ECN : CNP (50 : 50)	25	13.18	0.76	56.8	5.67
ECN : CNP (30 : 70)	31.6	13.37	0.79	62.8	6.64
CNP	28.5	13.76	0.81	65.4	7.30
Pt	NA	13.60	0.83	66.5	7.50

$J_{\text{sc}}$ , Short circuit current density or photo-current per unit area;  $V_{\text{oc}}$ , Open circuit voltage, that is, the potential developed in the external circuit on exposure of the DSSC to radiation; FF, Fill factor, which is the ratio of the maximum power obtained by the device and the theoretical power output possible by the device,  $\eta$ , Overall power conversion efficiency; ECN, Electrospun carbon nanofibres; CNP, Carbon nanoparticles; Pt, Platinum.

Pt CEs, indicating a potential of multi-walled CNTs for use in DSSC counter electrodes. Thapa *et al.*<sup>17</sup> fabricated CES using various weight ratios of carbon nanoparticles (CNPs) and electrospun carbon nanofibers (ENCs). CNPs were selected for their high specific surface area and ECNs were chosen due to their high electric conductivity. Both materials were easily available, cost-effective and offered good resistance to corrosion by  $\Gamma/\text{I}_3^-$  electrolyte. The conductivity of CEs increased consistently with 0%, 30%, 50%, 70% and 100% weight ratios of the ECNs to the CNPs, with a conductivity for the 100% ECN CE being 838 S/m. According to Thapa *et al.*<sup>17</sup>, analysis of cyclic voltammogram (CV) curves, which are a measure of the reduction of the redox electrolyte, indicated an increase in efficiency for greater weight ratios of CNPs. Despite these mutually contradicting finds, a higher CNP to ECN ratio was found to be more favourable after consideration of various parameters, as shown in Table 1. CEs with 100% CNPs out-performed those with 100% ECNs for all the photovoltaic parameters of  $V_{\text{oc}}$ ,  $J_{\text{sc}}$ , FF and overall PCE. According to the experimenters<sup>17</sup>, a reduction of charge transfer at the interface of the CE and the electrolyte, and a more efficient catalytic reduction of the  $\Gamma/\text{I}_3^-$  electrolyte for a higher CNP ratio dominated the increased charge conductivity caused by higher percentage of ECNs, resulting in their better efficiencies.

There has been extensive research on application of graphene and its compounds for the fabrication of CEs of DSSCs. Wang and Hu<sup>18</sup> have reported efficiencies attained from 0.7% to 6.8% in the early attempts at fabrication of CEs using graphene and its derivatives. However, in a more recent study, Gratzel *et al.*<sup>19</sup> achieved efficiencies as high as 9.54% by fabrication of CEs by coating a film of two-dimensional GO on cationic polydiallyldimethylammonium chloride (PDA) polymer by application of layer-by-layer arrangement. The unique energy band of GO along with its high specific surface area and electrical conductivity have been put to use in the fabrication of DSSCs, boosting the confidence in the potential of graphene and its various compounds in the area. In addition to the aforementioned carbonaceous materials, there has also been significant research employing conductive

polymers and various nanohybrids in CEs which have been discussed by Yun *et al.*<sup>20</sup>.

Besides carbonaceous materials, certain other alternatives to Pt for fabrication of DSSC CEs have also been explored. Wu *et al.*<sup>21</sup> studied the application of compounds of early transition metal (Ti, V, Mo, etc.) such as transition metal carbides (TMCs), transition metal nitrides (TMNs) and transition metal oxides (TMOs) in DSSC CEs. These compounds were chosen due to their durability, good electrical conductivity and importantly, their catalytic activity which was found to be at par with Pt. TMCs, TMNs and TMOs displayed good catalytic activity closely resembling that of Pt and superior to the respective pure metals, a property attributed to the alteration of the electronic structure of the metal due to the alien C or N atoms. The photovoltaic parameters of the so-formed DSSCs as noted by Wu *et al.*<sup>21</sup> are given in Table 1. It can be seen from the table that an appreciable PCE of 7.63% was achieved by a CE fabricated with VC–MC compared to the 7.5% PCE of a similar Pt-based CE. Also, the TMCs were found to have an inherently high corrosion resistance and excellent stability indicating the feasibility of application of these compounds in DSSCs.

Use of bifacial DSSCs is an up-and-coming improvement in conventional DSSCs in terms of increasing energy conversion-to-cost ratio. According to the traditional design, a considerable fraction of the incoming solar radiation and a small amount of dye molecules that are farthest from the transparent FTO–glass substrate are wasted, due to lack of contact with each other. This is because, after penetrating the transparent FTO–glass substrate, the radiation is absorbed by the layers of dye molecules in more immediate contact with it and hence dye molecules remain unexposed. However, if the sunlight that goes unused around the edges of the DSSC is reflected and sent to these layers of dye molecules through the counter electrode, an enhancement in efficiency can be achieved. This can be done with the use of mirrors or other light reflecting surfaces at the rear side of the DSSC, and calls for the use of such materials for the counter electrode that are transparent or

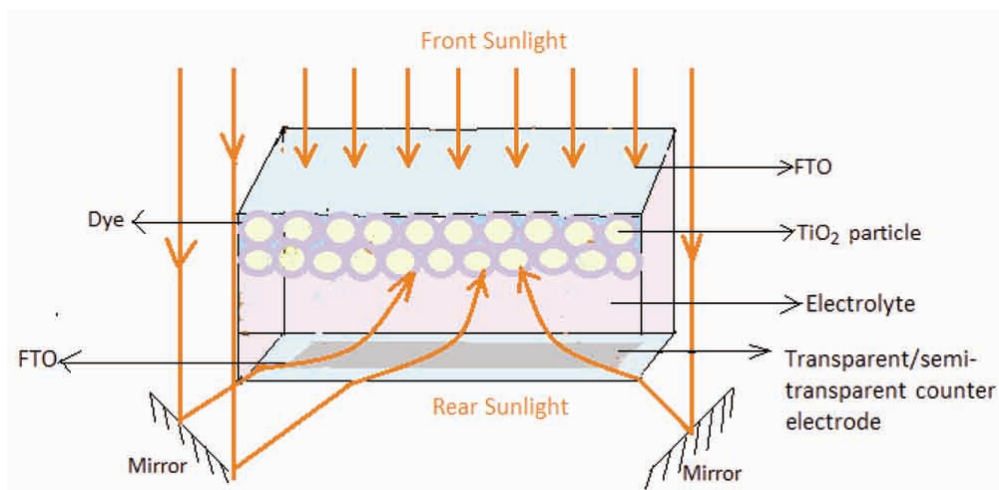


**Figure 4.** Schematic representation of a bifacial DSSC. Straight and flowing lines indicate the solar radiation.

semi-transparent. Figure 4 shows a schematic of such a bifacial DSSC.

Thus for bifacial DSSCs the frontal power conversion efficiency ( $PCE_{\text{front}}$ ) and the rear power conversion efficiency ( $PCE_{\text{rear}}$ ) together constitute the overall energy conversion efficiency, and a higher  $PCE_{\text{rear}}/PCE_{\text{front}}$  ratio is a measure of efficiency of the bifacial design of the DSSC.

Attempts have been made to modify Pt CEs by adding dopants that render the counter electrode semi-transparent or transparent as necessary for their application in bifacial DSSCs. This process also results in reduction in the amount of platinum required for the fabrication of CE, which is supposed to bring down the cost to some extent. Gurung *et al.*<sup>22</sup> fabricated a transparent CE using a composite of platinum with aluminium doped with zinc oxide (Pt/AZO). CV curve analysis was conducted by Gurung *et al.*<sup>22</sup> which indicated that the use of AZO with Pt in the composite did not result in any significant decrement in its performance as an electrocatalyst to regenerate the  $\Gamma^-/I_3^-$  electrolyte. They claimed transmittance values of 0.74–0.75 of the Pt–AZO composite counter electrode as opposed to a value of 0.63 of the one with pure Pt. The increase in transparency of the counter electrode was indicated to result in an increase in the value of  $J_{\text{sc}}$  and also that of  $PCE_{\text{rear}}$  of the bifacial DSSC opposed to a conventional DSSC of similar fabrication. The  $PCE_{\text{front}}$  value was found to decrease slightly, believed to have resulted due to a reduction in  $J_{\text{sc,front}}$  caused by the additional contribution of the AZO dopant to the resistance to the electron transport between the CE and  $\Gamma^-/I_3^-$  redox electrolyte. A higher  $PCE_{\text{rear}}/PCE_{\text{front}}$  ratio was obtained for a composite of Pt : AZO ratio of 2 : 1, which was used to suggest the possibility of application of such composites for fabrication of effective bifacial DSSCs. Iefanova *et al.*<sup>23</sup> presented an innovative way of application of DSSCs fabricated from transparent Pt-based CEs. They used

spray coating technology for coating hot ITO glass substrate with Pt NPs. This process was claimed to result in large cost reduction, by lowering Pt consumption by 86%, while at the same time fabricating CEs with 88% transparency. The resulting Pt NPs on ITO substrate CE were claimed to perform moderately well as an electrocatalyst for the  $\Gamma^-/I_3^-$  redox couple and amount to a DSSC with an overall PCE of 6.7%. However, Iefanova *et al.*<sup>23</sup>, instead of employing the transparent DSSC directly in a bifacial designed, presented an innovative employment of the same as a window-compatible photovoltaic. The transparent DSSCs were incorporated into window fittings for conversion of the incoming solar radiation into electrical energy, while at the same time reducing the costs of indoor cooling. This method represented the incorporation of transparent DSSCs into window-fitting photovoltaics, an arena of interest in the field of solar radiation harvesting and its conversion to electrical energy.

Alternative metals have also been explored to replace Pt in CEs of DSSCs. Bifacial DSSCs have been constructed employing transparent Ru–Se alloys in the CEs rendering optimal results of  $PCE_{\text{front}}$  and  $PCE_{\text{rear}}$  reaching as much as 8.76% and 5.90% respectively<sup>24</sup>. Results by another group indicated  $PCE_{\text{front}}$  and  $PCE_{\text{rear}}$  values of 6.21% and 4.72% respectively, for CuSe counter electrodes, going up to 7.81% and 5.38% for frontal and rear illuminations using alloys of CuSe with Co or Fe respectively<sup>25</sup>. Also, studies have been conducted recently on the application of the inexpensive polyaniline (PANI) and its composites as materials for construction of CEs in bifacial DSSCs. Tai *et al.*<sup>26</sup> fabricated a transparent CE for bifacial DSSC by *in situ* polymerization of aniline monomers directly on the FTO–glass substrate. The resulting bifacial DSSC displayed  $PCE_{\text{front}}$  and  $PCE_{\text{rear}}$  values corresponding to 6.54% and 4.26% respectively, comparable to the 6.69% overall efficiency of traditional

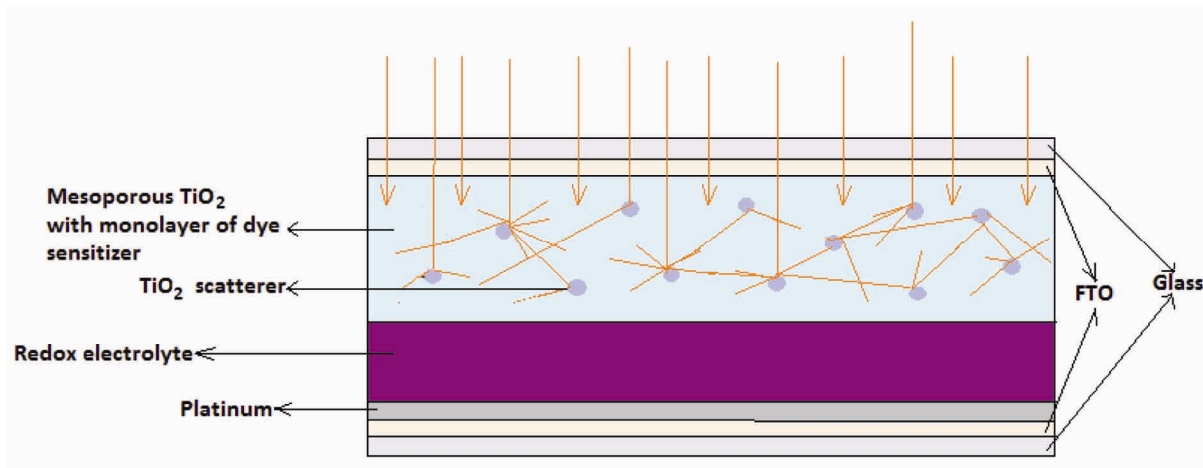


**Figure 5.** Schematic representation of a novel DSSC with internal scatterers for maximum illumination of dye sensitizers. Vertically downward facing arrows indicate incoming solar radiation. Short lines inside the DSSC indicate internally scattered light.

Pt-CE DSSC with all other factors being the same. Sun *et al.*<sup>27</sup> experimented on the preparation of flexible polyaniline/carbon composites for their application in bifacial DSSCs. The performance of PANI as an electrocatalyst in CE was found to be dependent on its idealized oxidation state, with emeraldine PANI displaying better performance than pernigraniline PANI. The CEs employing conducting emeraldine PANI as the electrocatalyst on a flexible graphite (FG) conducting substrate were shown to have 7.36% of overall energy conversion efficiency which was found comparable to the 7.45% efficiency of conventional DSSC with a Pt CE. The appreciable efficiency of the PANI composite was attributed to its excellent catalytic activity for reduction of the  $\Gamma/I_3^-$  electrolyte as well as high  $J_{sc}$  and FF values contributed by it due to low sheet resistance. More recent experiments by Wu *et al.*<sup>28</sup> showed a startling 8.35% efficiency of CEs fabricated with a PANI composite. Using 4-aminothiophenol (4-ATP) as a dopant, the PANI composite CE in fact was claimed to display a better potential for reduction of the  $\Gamma/I_3^-$  electrolyte than even Pt, making 4-ATP-doped PANI a better electrocatalyst than Pt in DSSC CEs. The efficiency of the device thus obtained has been claimed to be highest among the bifacial DSSCs fabricated with PANI CEs, even higher than bifacial DSSCs with modified Pt with an optimal efficiency of 7.46%. These studies indicate that PANI could be a potential candidate in the future as a material of construction of CEs in bifacial DSSCs, along with providing for cost-effectiveness.

A recent innovation has been made by Miranda-Munoz *et al.*<sup>29</sup>, wherein optimal illumination of the dye molecules has been achieved without the need for the rear-side illumination using bifacial designs. This method employed multiple scattering of light within the cell by randomized incorporation of dielectric TiO<sub>2</sub> scatterers in the mesoporous TiO<sub>2</sub> layer harbouring the dye molecules.

Figure 5 shows a schematic of the DSSC fabricated by the said method.

The incorporation of TiO<sub>2</sub> scatterers was to facilitate multiple scattering of light thus increasing its path length inside the cell, ensuring exposure of greater number of dye molecules to radiation to lead to higher photon-to-electron conversion. Furthermore, incorporation of the scatterers was found to result in no negative influence on the charge transport or the electrical properties of the cell, in fact leading to an increase in the photocurrent generated, with an averaged  $J_{sc}$  value of 13.54 mA/cm<sup>2</sup> and an overall cell efficiency of 6.7%. The study suggested a competition of such designs with bifacial designs in increasing photoconversion efficiency by effective illumination of the dye molecules calling for future explorations in the area.

## Discussion and conclusion

In this article, recent advances in the optimization of and modifications in the existing designs of photoanodes and counter electrodes of DSSCs have been discussed along with their impact on overall photovoltaic functions of DSSCs. With the growing importance of DSSCs as replacements for conventional Si-based solar cells, the importance of research and development over increasing the efficiency of their components, especially the electrodes, cannot be overstated. A lot of current research endeavours are being directed towards the replacement of Pt in the counter electrodes with more sustainable and economic alternatives. Efforts are also being directed towards replacement of TiO<sub>2</sub> with other semiconductors with greater stability under UV radiation. Bifacial DSSCs with transparent electrodes, to derive most from the incoming solar radiation, have also been designed. Alternatively, effective utilization of front-side illumination by

incorporation of internal scatterers has also been attempted, as has the innovative employment of transparent DSSCs into window photovoltaics. All these constitute recent innovations involving the electrodes of DSSCs which have been duly reviewed in this article, along with some insights into the shortcomings of current research, and the direction needed to be taken in the future. Exhaustive research with respect to these aspects of DSSCs would be important to make the technology large scale and sustainable.

- Graetzel, M. *et al.*, A low-cost, high-efficiency solar cell based on dye-sensitized colloidal TiO<sub>2</sub> films. *Nature*, 1991, **353**, 737–740.
- Hagfeldt, *et al.*, Dye-sensitized solar cells. *Chem. Rev.*, 2009, **110**, 6595–6663.
- Graetzel, M. *et al.*, Dye-sensitized solar cells: a brief overview. *Sol. Energy*, 2011, **85**, 1172–1178.
- Kang, *et al.*, Design and optimization of larger-sized dye-sensitized solar cell (DSSC), IEEE Conference Publications, 2010.
- Mehmood, *et al.*, Improvement in photovoltaic performance of dye-sensitized solar cell using activated carbon-TiO<sub>2</sub> composites based photoanode. *IEEE J. Photovolt.*, 2016, **6**, 1191–1195.
- Chou, *et al.*, Effect of different graphene oxide contents on dye-sensitized solar cells. *IEEE J. Photovolt.*, 2015, **5**(4), 1106–1112.
- Yao, *et al.*, Reduced interfacial recombination in dye-sensitized solar cells assisted with NiO : Eu<sup>3+</sup>, Tb<sup>3+</sup> coated TiO<sub>2</sub> film. *Sci. Rep.*, 2016, **6**, 31123.
- Sigdel, *et al.*, Dye-sensitized solar cells based on porous hollow tin oxide nanofibers. *IEEE Trans. Electron. Devices*, 2013, **62**(6), 2027–2032.
- Song, *et al.*, A simple self-assembly route to single crystalline SnO<sub>2</sub> nanorod growth by oriented attachment for dye-sensitized solar cells. *Nanoscale*, 2013, **5**, 1188–1194.
- Wang, *et al.*, Fabrication of a double layered photoanode consisting of SnO<sub>2</sub> nanofibers and nanoparticles for efficient dye-sensitized solar cells. *RSC Adv.*, 2013, **3**, 13804–13810.
- Gao, *et al.*, ZnO nanocrystalline aggregates synthesized through interface precipitation for dye-sensitized solar cells. *Nano Energy*, 2012, **2**, 40–48.
- Concina, *et al.*, Metal oxide semiconductors for dye-and quantum-dot-sensitized solar cells. *Small*, 2014, **2**–28.
- Yu, *et al.*, Indium tin oxide as a semiconductor material in efficient p-type dye-sensitized solar cells. *NPG Asia Materials*, 2016, **8**.
- Alibabaei, *et al.*, Applications of metal oxide materials in dye-sensitized photoelectrosynthesis cells for making solar fuels: let the molecules do the work. *J. Mater. Chem. A*, 2013, **1**, 4133–4145.
- Kouhnavard, *et al.*, Carbonaceous materials and their advances as a counter electrode in dye-sensitized solar cells, challenges and prospects. *ChemSusChem*, 2015, **8**, 1510–1533.
- Ramasamy, E. *et al.*, Efficient dye-sensitized solar cells with catalytic multiwall carbon nanotube counter electrodes. *ACS Mater. Interfaces*, 2009, **1**, 1145–1149.
- Thapa, A. *et al.*, Evaluation of counter electrodes composed by carbon nanofibers and nanoparticles in dye-sensitized solar cells. *IEEE Trans. Electron. Devices.*, 2013, **60**(11), 3883–3887.
- Wang, H. and Hu, Y.-H., Graphene as a counter electrode material for dye-sensitized solar cells. *Energy Environ. Sci.*, 2012, **5**, 8182–8188.
- Gratzel, M. *et al.*, Electrochemically reduced graphene oxide multilayer films as efficient counter electrode for dye-sensitized solar cells. *Sci. Rep.*, 2013, **3**, 1489.
- Yun, S., Hagfeldt, A. and Ma, T., Pt-free counter electrode for dye-sensitized solar cells with high efficiency. *Adv. Mater.*, 2014, **26**, 6210–6237.
- Wu, *et al.*, Economical Pt-free catalysts for counter electrodes of dye-sensitized solar cells. *J. Am. Chem. Soc.*, 2012, **134**, 3419–3428.
- Gurung, *et al.*, A simple cost-effective approach to enhance performance of bifacial dye-sensitized solar-cells. *IEEE J. Photovoltaics*, 2016, **6**, 912–917.
- Iefanova, *et al.*, Transparent platinum counter electrode for efficient semi-transparent dye-sensitized solar cells. *Thin Solid Films*, 2014, **562**, 578–584.
- Cai, *et al.*, Bifacial dye-sensitized solar cells with enhanced rear efficiency and power output. *Nanoscale*, 2014, **6**, 15127–15133.
- Li, P. and Tang, Q., Highly transparent metal selenide counter electrodes for bifacial dye-sensitized solar cells. *J. Power Sources*, 2016, **317**, 43–48.
- Tai, *et al.*, *In situ* prepared transparent polyaniline electrode and its application in bifacial dye-sensitized solar cells. *Nanoscale*, 2011, **5**, 3795–3799.
- Sun, *et al.*, *In situ* preparation of a flexible polyaniline/carbon composite counter electrode and its application in dye-sensitized solar cells. *J. Phys. Chem. C*, 2010, **114**, 11673–11679.
- Wu, *et al.*, Bifacial dye-sensitized solar cells: a strategy to enhance overall efficiency based on transparent polyaniline electrode. *Sci. Rep.*, 2014, **4**, 4028.
- Miranda-Munoz, *et al.*, Efficient bifacial dye-sensitized solar cells through disorder by design. *J. Mater. Chem. A*, 2016, **4**, 1953–1961.

ACKNOWLEDGEMENT. We thank the staff of the Institute of Chemical Technology, Mumbai for support.

Received 5 April 2017; revised accepted 22 May 2017

doi: 10.18520/cs/v113/i02/228-235